Article:
Lorent, Christian, Katz, Sagie, Duan, Jifu et al. (9 more authors) (2020) Shedding Light on Proton and Electron Dynamics in [FeFe] Hydrogenases. Journal of the American Chemical Society. pp. 5493-5497. ISSN 1520-5126

https://doi.org/10.1021/jacs.9b13075

Shedding light on proton and electron dynamics in [FeFe] hydrogenases

Christian Lorent[a], Sagie Katz[a], Jifu Duan[b], Catharina Kulka[a], Giorgio Caserta[a], Christian Teutloff[c], Shanika Yadav[e], Ulf-Peter Apfel[e,f], Martin Winkler[b], Thomas Happe[b], Marius Horch[a,d]*, Ingo Zebger[a]*

[a] Institut für Chemie, Technische Universität Berlin, Straße des 17. Juni 135, 10623 Berlin, Germany

[b] Faculty of Biology and Biotechnology, Photobiotechnology, Ruhr University Bochum, 44801 Bochum, Germany

[c] Fachbereich Physik, Freie Universität Berlin, Arnimallee 14, 14195 Berlin, Germany

[d] Department of Chemistry and York Biomedical Research Institute, University of York, Heslington, York, YO10 5DD, UK

[e] Inorganic Chemistry I, Ruhr University Bochum, Universitätsstr. 150, 44780 Bochum, Germany

[f] Department of Energy, Electrosynthesis group, Fraunhofer UMSICHT, Osterfelder Str. 3, 46047 Oberhausen, Germany

Supporting Information Placeholder

ABSTRACT: [FeFe] hydrogenases are highly efficient catalysts for reversible dihydrogen evolution. H_2 turnover involves different catalytic intermediates including a recently characterized hydride state of the active site (H-cluster). Applying cryogenic infrared and electron paramagnetic resonance spectroscopy to an [FeFe] model hydrogenase from *Chlamydomonas reinhardtii* (*Cr*HydA1), we have discovered two new hydride intermediates and spectroscopic evidence for a bridging CO ligand in two reduced H-cluster states. Our study provides novel insights into these key intermediates, their relevance for the catalytic cycle of [FeFe] hydrogenase, and novel strategies for exploring these aspects in detail.

[FeFe] hydrogenases are metalloenzymes that catalyze the reversible evolution of molecular hydrogen.[1] Their active site, called 'H-cluster', consists of a [2Fe] moiety and a [4Fe4S] cluster, which are covalently linked *via* a cysteinyl thiolate. H_2 turnover takes place at the [2Fe] subsite, which contains two iron ions that are coordinated by three CO and two CN^- ligands as well as an aza-dithiolate (ADT) bridge, which is involved in proton shuttling.[2–5]

During turnover, the H-cluster undergoes a series of redox transitions accompanied by proton translocation. The exact catalytic mechanism is still under debate, but several potential intermediates have been identified under steady-state conditions. The oxidized H_{ox} state features a paramagnetic, mixed-valence [$Fe^{I}Fe^{II}$] moiety and a diamagnetic, oxidized $[4Fe4S]^{2+}$ cluster.[6–9] One-electron reduction of H_{ox} yields two protomers, H_{red} and $H_{red}H^+$, that differ in the localization of the additional electron and a proton.[10–12] In H_{red}, the electron is stored at the reduced $[4Fe4S]^+$ site, while the localization of the proton is still under debate.[11,13] In $H_{red}H^+$, both the proton and the electron are transferred to the [2Fe] site, resulting in a [$Fe^{I}Fe^{I}$]-$[4Fe4S]^{2+}$ configuration and a protonated ADT bridge.[10–12] Addition of a second electron creates an [$Fe^{I}Fe^{I}$]-$[4Fe4S]^+$ state termed $H_{sred}H^+$.[12,14] This species has long been assumed to be in equilibrium with a hydride state that exhibits an [$Fe^{II}Fe^{II}$]-$[4Fe4S]^+$ configuration.[15,16] Recently, such a species, termed H_{hyd}, has been enriched by accumulating protons at the H-cluster, either by decreasing pH or by blocking intramolecular proton transfer from the active site.[17,18] Since these manipulations may affect the overall state of the enzyme in a complex manner, it is currently unclear if the detected H_{hyd} state represents a native catalytic intermediate and whether there may be other potentially relevant hydride states. Here, we use photoactivation in combination with cryogenic infrared (IR) and electron paramagnetic resonance (EPR) spectroscopy to study hydride states of an [FeFe] model hydrogenase from *Chlamydomonas reinhardtii* (*Cr*HydA1) without manipulating pH or the intramolecular proton transfer pathway.[11,19] This strategy yields detailed new insights into the structure and relevance of hydride states and other catalytic intermediates, thereby highlighting the potential of photoinduced cryo-spectroscopy for studying intermediates and transitions that are hard to probe under ambient steady state conditions.

H_2-reduced *Cr*HydA1 (pH 8.0), containing a mixture of H_{ox}, $H_{red}H^+$, H_{red}, and $H_{sred}H^+$ (Figure S1), was illuminated with blue light (460 nm) at 100 K. This treatment led to a photochemical transformation of the H-cluster, and the resulting light-*minus*-dark IR difference spectrum (Figure 1A) exhibits three negative CO stretching bands at 1922, 1881, and 1801 cm^{-1}, indicating a single parent state with one bridging and two terminal CO ligands (Figure 1C). Terminal CO stretch modes at 1922 and 1881 cm^{-1} identify this state as $H_{sred}H^+$,[14] and the lower-frequency signal at 1801 cm^{-1} indicates the presence of a bridging CO ligand in this species. While this feature is less prominent at room temperature, other IR markers of $H_{sred}H^+$ are hardly affected by temperature, which suggests that the bridging CO ligand is also present under ambient conditions but hardly detectable due to line broadening (Figure S2E). This statement is supported by IR spectra of *Cr*HydA1[12,20] as well as [FeFe] hydrogenases from *Clostridium acetobutylicum*[19] and *Thermotoga maritima*[21].

A new species, photochemically formed from $H_{sred}H^+$, is reflected by three positive signals in the light-*minus*-dark difference spectrum (Figure 1A), detected at 1972, 1954, and 1851 cm^{-1}. The dominant feature at 1954 cm^{-1} was previously assigned to $H_{sred}H^+$,[12,14] but our data confirm that this signal corresponds to a distinct state that is in equilibrium with $H_{sred}H^+$ at room temperature.[11]

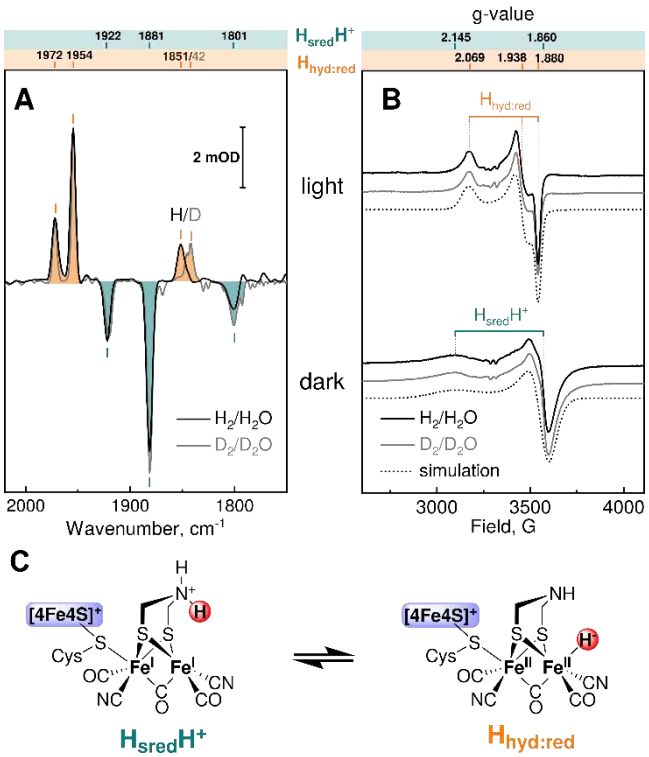

Figure 1. Photoconversion of $H_{sred}H^+$. (A) Light-*minus*-dark IR difference spectra of *Cr*HydA1 incubated with H_2 in H_2O (100 K, pH 8, black) and D_2 in D_2O (140 K, pD 8, grey). Signals reflect CO stretch modes. Difference spectra including the CN stretch region are depicted in Figure S5A. (B) Corresponding EPR spectra recorded at 10 K. Contributions from minor side species were subtracted as described in the (SI: Materials & Methods). EPR spectra obtained under H_2/H_2O (black) and D_2/D_2O (grey) are identical, but different $H_{sred}H^+/H_{hyd:red}$ ratios (Figure S2A and B) and photoconversion rates (Figure S3A, B) were observed. (C) Photoreaction between $H_{sred}H^+$ and $H_{hyd:red}$. Paramagnetic sites and the transferred hydrogen are highlighted in blue and red, respectively. IR absorbance and raw EPR spectra are shown in Figures S1 and S4, respectively.

Notably, the low-frequency mode of this photochemically enriched state (1851 cm^{-1}) indicates the presence of a bridging CO ligand (Figure 1C), and its overall IR signature suggests a structure similar but not identical to that of H_{hyd} (Figure S2E and Table S1),[15,17] as also noted recently.[20] To test this hypothesis, we next recorded light-*minus*-dark IR difference spectra of *Cr*HydA1 incubated with D_2 in D_2O (pD 8.0). Under these conditions, the band at 1851 cm^{-1} shifts towards lower frequencies (ca. 9 cm^{-1}), while no significant shift can be observed for the other bands (Figures 1A and S5; Table S1). This observation can be explained by the presence of a terminal hydride *trans* to the bridging CO ligand ligand,[15,17] and thus we assign the studied photoproduct to a new hydride species, called $H_{hyd:red}$ (Figures 1C and 3).

To gain more detailed insights into $H_{sred}H^+$ and $H_{hyd:red}$, we next recorded EPR spectra under conditions mimicking those of the IR experiments. According to room-temperature IR data, the H_2-reduced sample prepared for EPR spectroscopy is dominated by $H_{sred}H^+$ and H_{red} with traces of $H_{red}H^+$ and $H_{hyd:red}$ (Figure S2E, top trace). While H_{red} and $H_{red}H^+$ are net-diamagnetic,[10–12] $H_{sred}H^+$ [14] and $H_{hyd:red}$ are expected to yield signals from reduced [4Fe4S]$^+$ sites. EPR spectra of H_2-reduced *Cr*HydA1, recorded in the dark at 10 K, are dominated by a broad, almost axial signal (Figures 1B, bottom trace, and S2A; Table S2) and minor contributions from a more resolved rhombic species (Figures 1B, top trace, and S2A; Table S2). Upon prolonged illumination with blue light (120 min, 455 nm), the broad signal is almost completely converted to the rhombic species. Thus, in line with the IR data (Figure 1A), we assign the broad EPR signal to $H_{sred}H^+$ and the rhombic signature to $H_{hyd:red}$.

Strikingly, the broad axial species was previously observed for H_2-reduced *Cr*HydA1 and ascribed to an [Fe^IFe^I]-[4Fe4S]$^+$ species,[8,15] in line with our assignment to $H_{sred}H^+$. By contrast, a spectrum resembling the rhombic signature of $H_{hyd:red}$ was ascribed to $H_{sred}H^+$ in a pulsed EPR study performed at 10 K,[14] but our data suggest that the hydride tautomer rather than $H_{sred}H^+$ had been probed. This can be explained by coupling between the H-cluster subsites of $H_{sred}H^+$, which gives rise to fast spin relaxation (Figure S4A, B and E), so that $H_{sred}H^+$ may be easily missed in a mixture with the uncoupled rhombic $H_{hyd:red}$ signal (zero-spin [2Fe] subsite). Indeed, a distinct $H_{sred}H^+$ signal appears in X-band pulsed field-swept echo experiments only at temperatures below 10 K (Figure S4A inset), and the photoformation of $H_{hyd:red}$ under ambient light conditions may further complicate the detection of $H_{sred}H^+$ (Figure S3D and E). In line with our assignment, the rhombic $H_{hyd:red}$ signal is similar to the EPR spectrum of H_{hyd} (Figure S2C; Table S2).[15,16] Spectra, electron spin relaxation are not identical though (Figure S4A and E; Table S2), confirming that the two hydride states are distinct species.

Notably, H_{hyd} is mainly observed under proton-rich conditions (*vide supra*), and its CO/CN stretch frequencies are slightly higher than those of $H_{hyd:red}$.[17] In fact, IR differences between H_{hyd} and $H_{hyd:red}$ resemble those between species that differ by a proton presumably located at the [4Fe4S] cluster ($H_{ox}/H_{ox}H$; H_{ox}-CO/H_{ox}H-CO; $H_{red}/H_{red}H$; Table S1).[13] Thus, we propose that H_{hyd} is protonated at or close to this subsite, while $H_{hyd:red}$ is formed from $H_{sred}H^+$ without changing the net charge and protonation state of the H-cluster. This implies that $H_{sred}H^+$ and $H_{hyd:red}$ (but not H_{hyd}) are tautomers that can be rapidly interconverted by shuttling a proton between the ADT bridge and the substrate binding site (Figure S5A).

Such a reaction should also be possible for $H_{red}H^+$ (Figure 2B), thereby forming another hydride state. To accumulate this unobserved species, we next explored the light-sensitivity of $H_{red}H^+$. Here, the parent state was enriched by reducing *Cr*HydA1 with H_2/D_2 in H_2O/D_2O at pH/pD 6.0 (Figure 2A) prior to blue-light illumination (460 nm, 90 K). The most prominent negative band in the resulting light-*minus*-dark IR difference spectrum, detected at 1891 cm^{-1}, was previously assigned to $H_{red}H^+$.[12] Hence, the other two negative signals at 1919 and 1817 cm^{-1} can be ascribed to this H-cluster intermediate (Table S1). As for $H_{sred}H^+$, the presence of a bridging CO ligand (Figure 2B) is confirmed by the latter low-frequency band,[19,22] which is, again, weaker at room temperature for *Cr*HydA1 (Figure S2E, bottom traces). The $H_{red}H^+$-derived photoproduct can be identified by positive CO stretching bands at 1983, 1954, and 1865 cm^{-1} (Figure S2A). The latter feature indicates the presence of a bridging CO ligand, and its H/D exchange sensitivity (7 cm^{-1} shift) proves that the probed state represents a so-far unknown hydride species. In line with the structures and redox levels of the parent states, CO stretching frequencies of this diamagnetic (Figures S2C, S2D, and S3C) species are higher than those of $H_{hyd:red}$ (Figures 1A and 2A), allowing assignment to an analogous but one-electron oxidized hydride state, called $H_{hyd:ox}$ (Figures 2B and 3).

We used light-induced difference spectroscopy under cryogenic conditions to characterize transient H-cluster intermediates of an [FeFe] model hydrogenase. In contrast to studies at room temperature, this strategy allowed to explore short-lived species, without exchanging amino acids or invoking highly acidic conditions, both of which may interfere with the overall state of the target in an unpredictable manner.

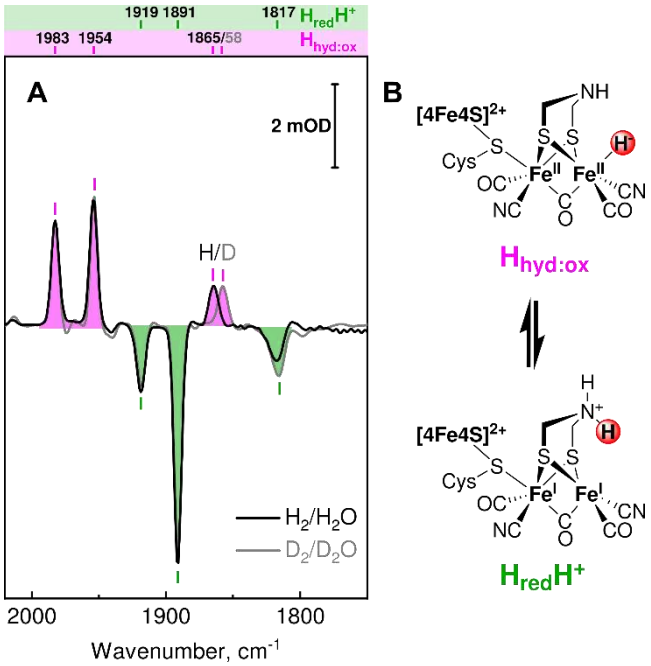

Figure 2. Photoconversion of $H_{red}H^+$. (A) Light-*minus*-dark IR difference spectra of *Cr*HydA1 (90 K), incubated with H_2 in H_2O (pH 6, black) and D_2 in D_2O (pD 6, grey). Contributions from $H_{sred}H^+$ and $H_{hyd:red}$ have been subtracted (SI: Materials & Methods). Signals reflect CO stretch modes. Difference spectra including the CN stretch region are depicted in Figure S5B. (B) Photoreaction between $H_{red}H^+$ and $H_{hyd:ox}$. The transferred hydrogen is highlighted in red. IR absorbance spectra are shown in Figure S1.

Specifically, we have analyzed two reduced H-cluster states, $H_{red}H^+$ and $H_{sred}H^+$, together with their previously unknown photo-enriched tautomers (Figure 3). In line with other recent studies, the two parent states were shown to carry bridging CO ligands,[20] which contradicts earlier reports claiming that $H_{red}H^+$ and $H_{sred}H^+$ feature bridging hydrides.[23,24] Thus, both reduced states can be converted to other catalytic intermediates without major structural rearrangement, indicating that they are indeed kinetically competent and likely involved in catalytic H_2 turnover.[25] Revising the EPR signature of $H_{sred}H^+$, we also found hints for interactions between the two H-cluster subsites, thereby indirectly confirming the non-zero-spin character of both [2Fe] and [4Fe4S] moieties of this species.

Photo-enriched tautomers of $H_{red}H^+$ and $H_{sred}H^+$ were accumulated at cryogenic temperatures, indicating low barriers towards their parent states and, thus, kinetic competency. Both photo states contain bridging CO ligands and a terminal hydride that is most likely formed from a protonated ADT bridge in their parent states, thereby supporting this feature and overall similar structures for $H_{red}H^+$ and $H_{sred}H^+$. Since the two parent states differ by the redox state of the [4Fe4S] sub-cluster, which is oxidized (2+) in $H_{red}H^+$ and reduced (1+) in $H_{sred}H^+$, the derived hydride states can be identified as oxidized and reduced analogues, termed $H_{hyd:ox}$ and $H_{hyd:red}$. The latter species is similar to the known H_{hyd} state, but differences in CO/CN stretching frequencies indicate that H_{hyd} is protonated close to the [4Fe4S] sub-cluster while $H_{hyd:red}$ is not. Hence, $H_{hyd:red}$ likely precedes H_{hyd} in the H_2-evolution cycle (Figure 3), and the relevance of this new state is supported by its presence in ambient thermal equilibrium with $H_{sred}H^+$.[10] The second new hydride species, $H_{hyd:ox}$, has not been detected before. Being a tautomer of $H_{red}H^+$, it would occur earlier in the H_2 evolution cycle, indicating that catalysis may take different routes after $H_{red}H^+$. Specifically, $H_{hyd:ox}$ could open an alternative reaction channel between $H_{red}H^+$ and $H_{hyd:red}$ that is operative if electron transfer towards the H-cluster is rate-limiting.

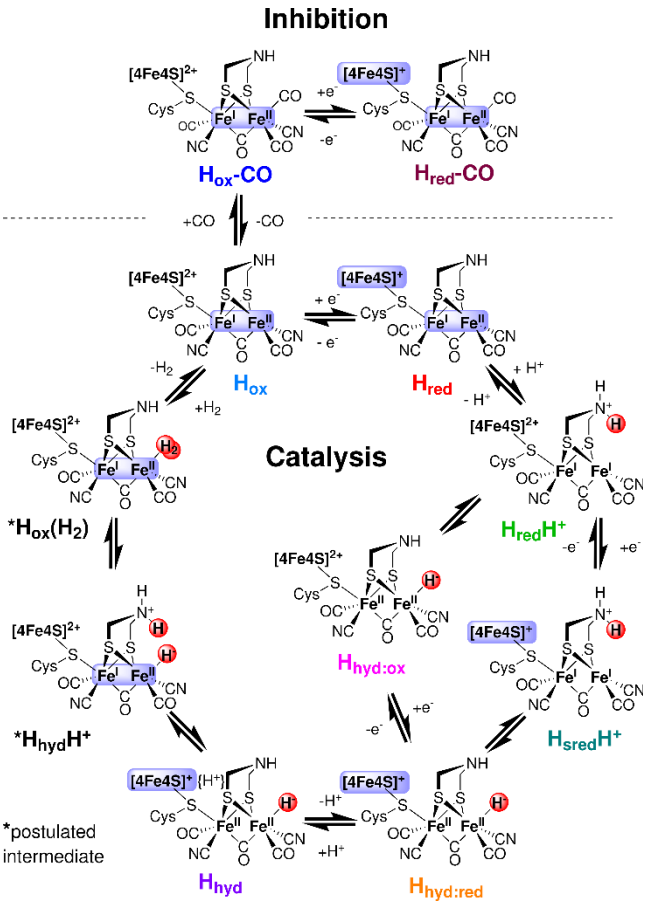

Figure 3. Proposed catalytic cycle. Paramagnetic sites and catalytically relevant hydrogens are highlighted in blue and red, respectively. Curly brackets indicate a proton at or close to the [4Fe4S] subsite.

In total, this study provides new avenues for understanding catalytic H_2 cycling by highlighting the enormous plasticity of the H-cluster towards proton and electron rearrangement and the multitude of kinetically competent states.[25] Moreover, our combination of cryo-spectroscopy and photoactivation strategies provides far-reaching new perspectives for the detection and characterization of missing links in the catalytic cycle of [FeFe] hydrogenases and other metalloenzymes.

ASSOCIATED CONTENT

Supporting Information

The Supporting Information is available free of charge on the ACS Publications website.

Material and methods; supporting IR and EPR data (PDF)

AUTHOR INFORMATION

Corresponding Authors

*marius.horch@york.ac.uk
*ingo.zebger@tu-berlin.de

ORCID

Christian Lorent 0000-0001-9057-4523
Jifu Duan 0000-0002-5158-2253
Giorgio Caserta 0000-0003-0986-3059
Shanika Yadav 0000-0003-1155-2241
Ulf-Peter Apfel 0000-0002-1577-242
Thomas Happe 0000-0003-1206-5234
Marius Horch 0000-0001-6656-1749
Ingo Zebger 0000-0002-6354-3585

Notes

The authors declare no competing financial interests.

ACKNOWLEDGMENT

The authors acknowledge Konstantin Laun and Prof. Dr. Peter Hildebrandt (TU Berlin) as well as Dr. James A. Birrell (MPI CEC) for helpful discussion. IZ is grateful for financial support by the DFG *via* the SPP 1927 "Iron-Sulfur for Life" (ZE 510/2-1, ZE 510/2-2). Des Weiteren gefördert durch die Deutsche Forschungsgemeinschaft (DFG) im Rahmen der Exzellenzstrategie des Bundes und der Länder – EXC 2008/1 – 390540038 (UniSysCat). The results were i.a. generated with the assistance of EU financial support (Article 38.1.2, GA) within the European Union's Horizon 2020 research and innovation program under grant agreement No 810856. IZ and GC acknowledge support by the Einstein Foundation within the EVF program for Steve Cramer. MH is grateful for financial support by the Leverhulme Trust (RPG-2018-188). UPA acknowledges financial support by the DFG (Emmy Noether grant AP242/2-1, the Cluster of Excellence RESOLV (EXC1069)) and the Fraunhofer Internal Programs under Grant No. Attract 097-602175. M. W. and T. H. are grateful for the financial support from the DFG, DFG Research Training Group GRK 2341 Microbial Substrate Conversion (Micon) and Volkswagen Stiftung (Design of [FeS] cluster containing Metallo-DNAzyme [Az93412]). Weitere Unterstützung erfolgte durch RESOLV, gefördert durch die DFG im Rahmen der Exzellenzstrategie des Bundes und der Länder – EXC2033 – Projektnummer 390677874.

REFERENCES

(1) Lubitz, W.; Ogata, H.; Rüdiger, O.; Reijerse, E. Hydrogenases. *Chem. Rev.* **2014**, *114*, 4081–4148.

(2) Silakov, A.; Wenk, B.; Reijerse, E.; Lubitz, W. ^{14}N HYSCORE Investigation of the H-Cluster of [FeFe] Hydrogenase: Evidence for a Nitrogen in the Dithiol Bridge. *Phys. Chem. Chem. Phys*. **2009**, *11* (31), 6592–6599.

(3) Berggren, G.; Adamska, A.; Lambertz, C.; Simmons, T. R.; Esselborn, J.; Atta, M.; Gambarelli, S.; Mouesca, J. M.; Reijerse, E.; Lubitz, W.; Happe, T.; Atero, V.; Fontecave, M. Biomimetic Assembly and Activation of [FeFe]-Hydrogenases. *Nature* **2013**, *499*, 66–69.

(4) Esselborn, J.; Lambertz, C.; Adamska-Venkatesh, A.; Simmons, T.; Berggren, G.; Noth, J.; Siebel, J.; Hemschemeier, A.; Artero, V.; Reijerse, E.; Fontecave, M.; Lubitz, W.; Happe, T. Spontaneous Activation of [FeFe]-Hydrogenases by an Inorganic [2Fe] Active Site Mimic. *Nat. Chem. Biol.* **2013**, *9*, 607–609.

(5) Esselborn, J.; Muraki, N.; Klein, K.; Engelbrecht, V.; Metzler-Nolte, N.; Apfel, U.-P.; Hofmann, E.; Kurisu, G.; Happe, T. A Structural View of Synthetic Cofactor Integration into [FeFe]-Hydrogenases. *Chem. Sci.* **2016**, *7*, 959-968.

(6) Pierik, A. J.; Hulstein, M.; Hagen, W. R.; Albracht, S. P. J. A Low-Spin Iron with CN and CO as Intrinsic Ligands Forms the Core of the Active Site in [Fe]-Hydrogenases. *Eur. J. Biochem*. **1998**, *258*, 572–578.

(7) Roseboom, W.; De Lacey, A. L.; Fernandez, V. M.; Hatchikian, E. C.; Albracht, S. P. J. The Active Site of the [FeFe]-Hydrogenase from *Desulfovibrio desulfuricans*. II. Redox Properties, Light Sensitivity and CO-Ligand Exchange as Observed by Infrared Spectroscopy. *J. Biol. Inorg. Chem.* **2006**, *11*, 102–118.

(8) Mulder, D. W.; Ratzloff, M. W.; Shepard, E. M.; Byer, A. S.; Noone, S. M.; Peters, J. W.; Broderick, J. B.; King, P. W. EPR and FTIR Analysis of the Mechanism of H_2 Activation by [FeFe]-Hydrogenase HydA1 from *Chlamydomonas reinhardtii*. *J. Am. Chem. Soc.* **2013**, *135*, 6921–6929.

(9) Reijerse, E. J.; Pelmenschikov, V.; Birrell, J. A.; Richers C. P.; Kaupp, M.; Rauchfuss, T. B.; Cramer, S. P.; Lubitz, W. Asymmetry in the Ligand Coordination Sphere of the [FeFe] Hydrogenase Active Site Is Reflected in the Magnetic Spin Interactions of the Aza-propanedithiolate Ligand. *J. Phys. Chem. Lett.* **2019**, *10*, 6794−6799

(10) Adamska-Venkatesh, A.; Krawietz, D.; Siebel, J.; Weber, K.; Happe, T.; Reijerse, E.; Lubitz, W. New Redox States Observed in [FeFe] Hydrogenases Reveal Redox Coupling within the H-Cluster. *J. Am. Chem. Soc.* **2014**, *136*, 11339–11346.

(11) Katz, S.; Noth, J.; Horch, M.; Shafaat, H. S.; Happe, T.; Hildebrandt, P.; Zebger, I. Vibrational Spectroscopy Reveals the Initial Steps of Biological Hydrogen Evolution. *Chem. Sci*. **2016**, *7*, 6746–6752.

(12) Sommer, C.; Adamska-Venkatesh, A.; Pawlak, K.; Birrell, J. A.; Rüdiger, O.; Reijerse, E. J.; Lubitz, W. Proton Coupled Electronic Rearrangement within the H-Cluster as an Essential Step in the Catalytic Cycle of [FeFe] Hydrogenases. *J. Am. Chem. Soc*. **2017**, *139*, 1440–1443.

(13) Senger, M.; Mebs, S.; Duan, J.; Shulenina, O.; Laun, K.; Kertess, L.; Wittkamp, F.; Apfel, U.-P.; Happe, T.; Winkler, M.; Haumann, M.; Stripp, S. T. Protonation/Reduction Dynamics at the [4Fe–4S] Cluster of the Hydrogen-Forming Cofactor in [FeFe]-Hydrogenases. *Phys. Chem. Chem. Phys.* **2018**. *20*, 3128-3140.

(14) Adamska, A.; Silakov, A.; Lambertz, C.; Rüdiger, O.; Happe, T.; Reijerse, E.; Lubitz, W. Identification and Characterization of the "Super-Reduced" State of the H-Cluster in [FeFe] Hydrogenase: A New Building Block for the Catalytic Cycle? *Angew. Chem. Int. Ed.* **2012**, *51*, 11458–11462.

(15) Mulder, D. W.; Ratzloff, M. W.; Bruschi, M.; Greco, C.; Koonce, E.; Peters, J. W.; King, P. W. Investigations on the Role of Proton-Coupled Electron Transfer in Hydrogen Activation by [FeFe]-Hydrogenase. *J. Am. Chem. Soc.* **2014**, *136*, 15394–15402.

(16) Mulder, D. W.; Guo, Y.; Ratzloff, M. W.; King, P. W. Identification of a Catalytic Iron-Hydride at the H-Cluster of [FeFe]-Hydrogenase. *J. Am. Chem. Soc.* **2017**, *139*, 83–86.

(17) Winkler, M.; Senger, M.; Duan, J.; Esselborn, J.; Wittkamp, F.; Hofmann, E.; Apfel, U. P.; Stripp, S. T.; Happe, T. Accumulating the Hydride State in the Catalytic Cycle of [FeFe]-Hydrogenases. *Nat. Commun*. **2017**, *8*, 1-7.

(18) Duan, J.; Senger, M.; Esselborn, J.; Engelbrecht, V.; Wittkamp, F.; Apfel, U. P.; Hofmann, E.; Stripp, S. T.; Happe, T.; Winkler, M. Crystallographic and Spectroscopic Assignment of the Proton Transfer Pathway in [FeFe]-Hydrogenases. *Nat. Commun.* **2018**, *9*, 1-11.

(19) Ratzloff, M. W.; Artz, J. H.; Mulder, D. W.; Collins, R. T.; Furtak, T. E.; King, P. W. CO-Bridged H-Cluster Intermediates in the Catalytic Mechanism of [FeFe]-Hydrogenase CaI. *J. Am. Chem. Soc.* **2018**, *140*, 7623–7628.

(20) Birrell, J. A.; Pelmenschikov, V.; Mishra, N.; Wang, H.; Yoda, Y.; Tamasaku, K.; Rauchfuss, T. B.; Cramer, S. P.; Lubitz, W.; DeBeer, S. Spectroscopic and Computational Evidence that [FeFe] Hydrogenases Operate Exclusively with CO-Bridged Intermediates. *J. Am. Chem. Soc.* **2020**, *142*, 222–232.

(21) Chongdar, N.; Birrell, J. A.; Pawlak, K.; Sommer, C.; Reijerse, E. J.; Rüdiger, O.; Lubitz, W.; Ogata, H. Unique Spectroscopic Properties of the H-Cluster in a Putative Sensory [FeFe] Hydrogenase. *J. Am. Chem. Soc.* **2018**, *140*, 1057–1068.

(22) Senger, M.; Eichmann, V.; Laun, K.; Duan, J.; Wittkamp, F.; Knör, G.; Apfel, U.-P.; Happe, T.; Winkler, M.; Heberle, J.; Stripp, S. T. How [FeFe]-Hydrogenase Facilitates Bidirectional Proton Transfer. *J. Am. Chem. Soc.* **2019**, *141*, 17394-17403.

(23) Mebs, S.; Senger, M.; Duan, J.; Wittkamp, F.; Apfel, U. P.; Happe, T.; Winkler, M.; Stripp, S. T.; Haumann, M. Bridging Hydride at Reduced H-Cluster Species in [FeFe]-Hydrogenases Revealed by Infrared Spectroscopy, Isotope Editing, and Quantum Chemistry. *J. Am. Chem. Soc.* **2017**, *139*, 12157–12160.

(24) Chernev, P.; Lambertz, C.; Brünje, A.; Leidel, N.; Sigfridsson, K. G. V.; Kositzki, R.; Hsieh, C. H.; Yao, S.; Schiwon, R.; Driess, M.; Limberg, C.; Happe, T.; Haumann, M. Hydride Binding to the Active Site of [FeFe]-Hydrogenase. *Inorg. Chem.* **2014**, *53*, 12164–12177.

(25) Sanchez, M. L. K.; Sommer, C.; Reijerse, E.; Birrell, J. A.; Lubitz, W.; Dyer, R. B. Investigating the Kinetic Competency of CrHydA1 [FeFe] Hydrogenase Intermediate States via Time-Resolved Infrared Spectroscopy. *J. Am. Chem. Soc.* **2019**, *141*, 16064-16070

SYNOPSIS TOC